

A UNITED STATES
DEPARTMENT OF
COMMERCE
PUBLICATION

NOAA Technical Report NOS 53

U.S. DEPARTMENT OF COMMERCE
National Oceanic and Atmospheric Administration
National Ocean Survey

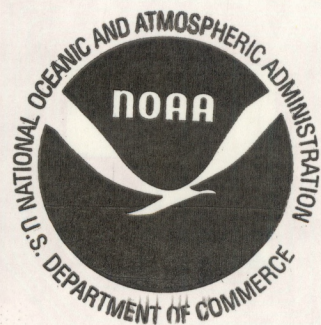
QC
801
U651
no. 53
c. 2

Grid Calibration by Coordinate Transfer

LAWRENCE FRITZ

December 1972

ROCKVILLE, MD.



NOAA TECHNICAL REPORTS

National Ocean Survey Series

Survey (NOS) provides charts and related information for the safe navigation of marine and air commerce. The earth science data—from geodetic, hydrographic, oceanographic, geomagnetic, seismologic, gravimetric, and tides, investigations, and measurements—to protect life and property and to meet the needs of engineering, navigation, and industrial interests.

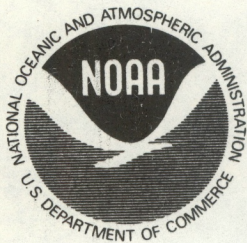
Because many of these reports deal with new practices and techniques, the views expressed are those of the authors, and do not necessarily represent final Survey policy. NOS series NOAA Technical Reports is a continuation of, and retains the consecutive numbering sequence of, the former series, ESSA Technical Report Coast and Geodetic survey (C&GS), and the earlier series, C&GS Technical Bulletin.

Reports in the series are available through the Superintendent of Documents, U.S. Government Printing Office, Washington, D.C. 20402. Those publications marked by an asterisk are out of print.

COAST AND GEODETIC SURVEY TECHNICAL BULLETINS

- *C&GS 1. Aerotriangulation Adjustment of Instrument Data by Computational Methods. William D. Harris, January 1958. (Superseded by No. 23.)
- *C&GS 2. Tellurometer Traverse Surveys, Lt. Hal P. Demuth, March 1968.
- *C&GS 3. Recent Increases in Coastal Water Temperature and Sea Level—California to Alaska. H. B. Stewart, Jr., B. D. Zetler, and C. B. Taylor, May 1958.
- *C&GS 4. Radio Telemetry Applied to Survey Problems. Richard R. Ross, February 1959.
- *C&GS 5. Raydist on Georges Bank. Capt. Gilbert R. Fish, April 1959.
- *C&GS 6. The Tsunami of March 9, 1957, as Recorded at Tide Stations. Garrett G. Salsman, July 1959.
- *C&GS 7. Pantograph Adjustment. G. C. Tewinkel, July 1959.
- *C&GS 8. Mathematical Basis of Analytic Aerotriangulation. G. C. Tewinkel, August 1959. (Superseded by No. 21.)
- *C&GS 9. Gravity Measurement Operations in the Field. Lt. Comdr. Hal P. Demuth, September 1959.
- *C&GS 10. Vertical Adjustment of Instrument Aerotriangulation by Computational Methods. William B. Harris, September 1959. (Superseded by No. 23.)
- *C&GS 11. Use of Near-Earth Satellite Orbits for Geodetic Information. Paul D. Thomas, January 1960.
- *C&GS 12. Use of Artificial Satellites for Navigation and Oceanographic Surveys. Paul D. Thomas, July 1960.
- C&GS 13. A Singular Geodetic Survey. Lansing G. Simmons, September 1960. Price \$0.15.
- *C&GS 14. Film Distortion Compensation for Photogrammetric Use. G. C. Tewinkel, September 1960.
- *C&GS 15. Transformation of Rectangular Space Coordinates. Erwin Schmid, December 1960.
- *C&GS 16. Erosion and Sedimentation—Eastern Chesapeake Bay at the Choptank River. G. F. Jordan, January 1961.
- *C&GS 17. On the Time Interval Between Two Consecutive Earthquakes. Tokuji Otsu, February 1961.
- *C&GS 18. Submarine Physiography of the U.S. Continental Margins. G. F. Jordan, March 1962.
- *C&GS 19. Analytic Absolute Orientation in Photogrammetry. G. C. Tewinkel, March 1962.
- *C&GS 20. The Earth as Viewed from a Satellite. Erwin Schmid, April 1962.
- *C&GS 21. Analytic Aerotriangulation. W. D. Harris, G. C. Tewinkel, and C. A. Whitten, July 1963. (Corrected July 1963.)
- *C&GS 22. Tidal Current Surveys by Photogrammetric Methods. Morton Keller, October 1963.
- *C&GS 23. Aerotriangulation Strip Adjustment. M. Keller and G. C. Tewinkel, August 1964.
- *C&GS 24. Satellite Triangulation in the Coast and Geodetic Survey. February 1965.
- *C&GS 25. Aerotriangulation: Image Coordinate Refinement. M. Keller and G. C. Tewinkel, March 1965.
- *C&GS 26. Instrumented Telemetering Deep Sea Buoys. H. W. Straub, J. M. Arthaber, A. L. Copeland, and D. T. Theodore, June 1965.
- *C&GS 27. Survey of the Boundary Between Arizona and California. Lansing G. Simmons, August 1965.
- *C&GS 28. Marine Geology of the Northeastern Gulf of Maine. R. J. Malloy and R. N. Harbison, February 1966.
- *C&GS 29. Three-Photo Aerotriangulation. M. Keller and G. C. Tewinkel, February 1966. Price \$0.35.
- *C&GS 30. Cable Length Determinations for Deep-Sea Oceanographic Operations. Capt. Robert C. Darling, June 1966.
- *C&GS 31. The Automatic Standard Magnetic Observatory. L. R. Alldredge and I. Saldukas, June 1966.

(Continued on inside back cover)



U.S. DEPARTMENT OF COMMERCE
Peter G. Peterson, Secretary

NATIONAL OCEANIC AND ATMOSPHERIC ADMINISTRATION
Robert M. White, Administrator

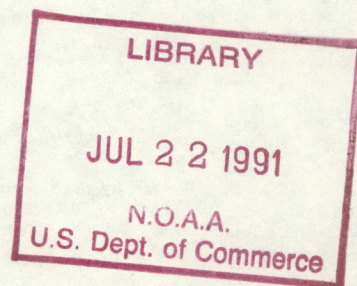
NATIONAL OCEAN SURVEY
Allen L. Powell, Director

NOAA Technical Report NOS 53

Grid Calibration by Coordinate Transfer

Lawrence Fritz

ROCKVILLE, MD.
DECEMBER 1972

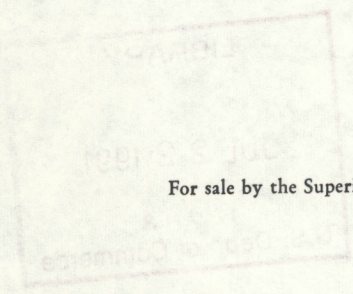


U.S. DEPARTMENT OF COMMERCE
Peter G. Peterson, Secretary
NATIONAL OCEANIC AND ATMOSPHERIC ADMINISTRATION
Robert M. White, Administrator
NATIONAL OCEAN SURVEY
Allen L. Powell, Director



UDC 528.165:528.235:528.35

528	Geodesy. Cartography
.1	Adjustment of errors
.165	Graphical adjustment
.235	Grids
.35	Trilateration



For sale by the Superintendent of Documents, U.S. Government Printing Office, Washington, D.C. 20402.
Price \$.40 domestic postpaid or \$.30 G.P.O. Bookstore.

NOAA Technical Report NOS 83
DECEMBER 1952

CONTENTS

	Page
Abstract	1
Introduction	1
The coordinate transfer method	2
Grid 1320—a test calibration	4
Accuracy determination	9
Grid accuracy formula development	10
Accuracy determination for grid 1320	13
Grid 773—a trilateration comparison	15
Conclusions and recommended improvements	20
Acknowledgments	20
References	20

Grid Calibration by Coordinate Transfer

LAWRENCE W. FRITZ

*National Ocean Survey, NOAA
Rockville, Md.*

ABSTRACT. An operational technique is described for providing precise grid coordinates for an uncalibrated grid. The demand for calibrated grids to provide quality control of two-axis comparators has increased substantially by the rapid international growth of analytical photogrammetry.

For the grid calibration technique termed "coordinate transfer," a precisely calibrated Master grid is used as a reference standard from which a second-generation calibrated grid may be obtained. The inherent two-dimensional geometric strength, as well as the absolute scale of the Master, is transferred to the uncalibrated grid in a manner similar to the method employed in the transferring of absolute scale from a precisely calibrated linear scale to a grid in the trilateration technique of grid calibration. Test results and relative accuracies of two grid calibration methods are discussed.

INTRODUCTION

The primary use of a precisely calibrated grid plate is to provide a standard for the metric calibration of two-axis precision comparators. Such use improves the attainable coordinate measurement accuracy of the comparators. The use of a precision *X, Y* grid plate rather than a precision linear scale for comparator calibration is justified by the realization that the redundancy of grid intersections will enhance the validity of the calibration. More importantly, the use of a grid will permit determination of the skewness of the axes and the degree, if any, of interdependence of the axes as a part of the calibration.

Grid calibration is the determination of the absolute rectangular coordinate positions of selected grid line intersections of a glass grid plate. The ideal method of determination is to apply the principle of trilateration (Malhotra 1968, Poetzschke 1967). By this method, a series of independent diagonal and side-length distance measurements between the selected grid intersections are compared with their corresponding distance measure-

ments on a precisely calibrated¹ glass scale. The measurements should be made on a 1-micrometer (μm) or better "least count" comparator. This "trilateration" method is considered a "null" method as it involves difference measurements only, which in effect virtually eliminate any personal, mechanical, or environmental biases.

The trilateration of a glass grid plate involves a minimum of 16 comparator pointings necessary to establish one distance (length) measurement; that is, four pointings at each end intersection of the grid length plus four pointings at each end tick of the corresponding linear-scale distance. This means that for a grid of 25 equally spaced selected intersections, a minimum of 2,560 pointings are required to provide the necessary 160 independently measured lengths. The measuring process is slowed considerably by the frequent shifting

¹The glass scale should be so precisely calibrated that it can be treated as absolute (errorless) in the ensuing trilateration adjustment.

of the glass scale. It is estimated that the minimum time required for a single operator to obtain a single set of measurements by this method is about 80 hours.

As a direct consequence of the tedious and time-consuming measuring technique involved in trilateration, the alternative coordinate transfer method was developed to succeed (but not to replace) it. The need for precisely calibrated plates has increased because of the increasing use of two-axis comparators; this need justified the development of the "coordinate transfer" method of grid calibration. This method takes advantage of the inherent two-dimensional geometrical strength, as well as the absolute scale of a precisely trilaterated grid in much the same way as trilateration uses the absolute scale of a calibrated glass scale. The effort expended using the coordinate transfer technique requires approximately 40 pointings per selected grid intersection; that is, for the Master calibrated grid plate and for the uncalibrated grid plate, a series of five direct pointings of the grid intersection for each of four plate rotations (cases) is recommended. This means that a minimum of only 1,000 pointings is required for a 25-intersection grid. A conservative time estimate for this measuring process is about 12 hours by one operator for a single set (eight cases) of measurements.

Advocates of both the trilateration and coordinate transfer methods recommend that three sets of measurements be performed, each by a different operator, for a truly complete grid calibration.

THE COORDINATE TRANSFER METHOD

The accuracy of this method is dependent primarily on the capabilities and stability of the comparator and the accuracy of the master grid coordinates used. The desirable basic comparator and environmental requirements are:

- (1) adherence to Abbe's comparator principle (Schwedefsky 1960) as closely as possible,
- (2) two mechanically independent axes,
- (3) least count of $1\ \mu\text{m}$ or better,
- (4) mechanically capable of $1\ \mu\text{m}$ or better accuracy after application of comparator calibration corrections, and
- (5) thermal stability during measuring period (3 days or more).

Measurement procedures recommended are a minimum of five pointings, preferably independent, per grid intersection. An additional closeout set of three pointings on the first grid intersection read is desirable to ensure comparator stability during the measurement period. When independent pointings are not possible, five replicative (International Society for Photogram-

metry 1964) pointings per intersection should be made, with additional replications, in groups of three, if the initial pointing spread exceeds $3\ \mu\text{m}$. Only obvious pointing blunders should be rejected by the operator.

The recommended measurement process requires each operator to measure a grid plate completely four times, once in each of four successive 90° rotations of the grid on the comparator. This procedure has the beneficial effects of:

- (1) minimizing any systematic residual comparator errors,
- (2) nullifying operator pointing biases, and
- (3) statistically improving the final result through redundancy of observations.

Experience has demonstrated that the use of three operators, each measuring four 90° cases, provides sufficient redundancy to ensure a valid set of accurate measurements of the grid. The use of three operators will tend to minimize the effects of personal errors as well as short-term residual biases of the comparator. All grid measurements should be made in as short a timespan as possible to minimize the influence of environmental and other time-related changes. The grid plates to be measured should be "seasoned" on the comparator before measurement to prevent dimensional changes of the grid during the initial measurement period.

The general procedure for measurement and data reduction is outlined by the following steps.

- (1) Have three operators each measure one set (four cases) of the Master (trilateration calibrated) grid. One case consists of measurements of all grid intersections in one plate position on the comparator. The grid must be rotated consecutively by 90° after each case to fulfill the set.
- (2) Determine the comparator calibration correction parameters from the measurements of the Master grid. These correction parameters should include as a minimum the three linear parameters: x -scale, y -scale, and lack-of-orthogonality-of-axes angle. Nonlinear correction parameters are also desirable, especially for lead-screw comparators.
- (3) Immediately following the Master grid measurements, have three operators measure the uncalibrated grid on the same comparator (one set each).
- (4) Apply the comparator calibration correction parameters to the uncalibrated grid measurements to obtain 12 cases of orthogonal grid coordinates.

- (5) Transform each case of grid coordinates into a common orientation system by performing a least-squares adjustment. This adjustment involves two translation parameters and one rotation parameter and is commonly called a two-dimensional Helmert transformation, or a center of gravity coordinate transformation. Choose an appropriate set of coordinates to be adjusted to for the common orientation system, such as ideal "square" coordinates (the manufacturer's intended coordinates). This step provides 12 cases of orthogonal grid coordinates in a common orientation system. An evaluation or plot of these 12 determinations provides a logical point for rejecting any previously undetected observation blunders.
- (6) Obtain the mean of the coordinates of each grid intersection to obtain a provisional set of grid values. When measuring operators are unequally skilled, a weighted mean set of grid coordinates should also be computed. The most appropriate choice of weights is the inverse of the pointing-precision-variance for each case, which is determined from the replicated comparator measurements. This may provide a more meaningful and compatible set of provisional grid values.
- (7) "Best fit" each case of grid coordinates (from either step 4 or step 5) to the provisional set of grid values, using the two-dimensional Helmert transformation. However, this time the adjustment should allow an overall scale change of each case. This is a smoothing process intended to remove additional systematic differences (primarily due to thermal effects) between cases of measurements.
- (8) Compute a coordinate standard deviation (m_{c_i}) for each of the newly oriented orthogonalized cases from the provisional mean set of grid values. These standard deviations provide an indication of the precision of the grid calibration. The pooled standard deviation (m_c) provides the grid calibration *precision*, as it is the standard error of an observation of unit weight for all 12 cases, assuming that all observations are of equal quality.

$$m_{c_i}^2 = \frac{\sum_{i=1}^p \left\{ (x_i - \bar{x}_i)^2 + (y_i - \bar{y}_i)^2 \right\}}{2(p-1)} \quad (1)$$

$$m_c^2 = \frac{\sum_{i=1}^n m_{c_i}^2}{n} \quad (2)$$

where: p = number of grid intersections,
 n = number of cases.

- (9) Obtain the mean of the 12 determinations of each grid intersection (from step 7) to obtain the final calibrated coordinate values of the grid. Again, make an auxiliary computation to obtain a weighted mean set of grid values. Appropriate weights should be chosen from the fit (m_{c_i}) of each of the 12 cases to the mean (provisional) set of grid values. This computation should provide more accurate calibrated grid values when the individual case determination variances, $m_{c_i}^2$, have a large dispersion.
- (10) Compute the precision statistics of the final mean (weighted) coordinates for each grid intersection and for all grid intersections (under the premise that they are all of equal quality). Make computations to include the standard deviation of a coordinate observation of unit weight (m_x, m_y), the standard deviation of a grid intersection observation of unit weight (m_{pt}), the standard deviation of weighted mean coordinate ($m_{\bar{x}}, m_{\bar{y}}$), and the standard deviation of weighted mean grid intersection ($m_{\bar{p}\bar{t}}$). (See equations (9) through (16)).

Some of the subtleties implied in the procedure are commented upon here.

The uncalibrated grid need not possess the same dimensions nor the same number of grid intersections as the Master grid used. However, the use of identically ruled grids placed in the same alignments on the comparator will greatly improve the validity of the comparator calibration corrections applied (step 2).

The transfer of the absolute scale of the Master grid to the uncalibrated grid is achieved by the application of the two scalars in step 4. The additional minor scaling of data (step 7) does not affect this transferred absolute scale, as the provisional set of grid values used for this scaling is at the mean scale of all 12 cases.

The accuracy of the final mean coordinates determined for the grid, in the limiting case, approaches the accuracy of the Master grid used. Therefore, the use of a highly accurate Master grid is desirable.

Another point to be emphasized is that although the outlined procedure provides a set of grid values possessing a high degree of internal precision, these values may be affected by an unremoved bias peculiar to the particular brand of comparator used. To determine whether any such biases exist, the entire procedure must be repeated on at least one *different* brand of comparator.

GRID 1320—A TEST CALIBRATION

A test calibration was performed to provide a comparison of the attainable accuracies of the "trilateration" and "coordinate transfer" grid calibration methods. The grid plate chosen for calibration was a standard Wild Stereocomparator grid plate (1320) that has finely engraved, 10- μm -wide grid lines spaced 1 cm apart over a 23- by 23-cm format. A set of 25 grid intersections, symmetrically spaced over a 20-cm square format with 5-cm spacing was selected for coordinate determination.

Grid 1320 was trilaterated (Poetzschke 1967) at the Ballistic Research Laboratories, Aberdeen, Md., in March 1967. The measurements were performed on a Wild Stereocomparator (STK-1) by one operator, using a calibrated 30-cm glass scale that has both 1-cm and $\sqrt{2}$ -cm graduation lines. The glass scale was calibrated by the Swiss Federal Bureau of Measures and Weights (at a temperature of 20°C), with a standard error of less than $\pm 1/2 \mu\text{m}$ for any graduation line.

In June 1969, grid 1320 was measured on a Mann two-axis monocomparator by three operators, each measuring four 90° rotation cases. Immediately following these measurements, the comparator was calibrated. This calibration was based on the measurement of the precisely calibrated grid 773 (Poetzschke 1967) by three operators, each measuring four 90° rotation cases. The Master grid 773 had been calibrated previously by a weighted mean of four complete sets of trilateration measurements made by four operators. The trilateration coordinates have been updated subsequently through evaluation of several years of comparator calibration measurements on several brands of comparators. The updated coordinate values of grid 773 have consistently demonstrated a coordinate standard error of less than $\pm 0.3 \mu\text{m}$.

In late June 1969, grid 1320 was measured on one stage of a Zeiss PSK stereocomparator by three operators, each measuring four 90° rotation cases. The PSK had been calibrated 15 months earlier in the same manner by Master grid 773. A recalibration of the PSK was not deemed necessary as its calibration remains valid for long time periods due to its design.

Data reduction of the Mann and PSK measurements was performed as outlined in the previous section. The

Mann monocomparator uses lead screws and slide-guiding ways that introduce nonlinear errors to the measurements. These nonlinear errors were removed from the grid measurements. The PSK measurements were refined by linear comparator corrections only.

On the Mann comparator, the measurement of the two grids (773 and 1320) took a total of 24 hours by five operators. (One operator measured both.) The PSK measurements of grid 1320 alone took a total of 30 hours by three operators. Allowing an equivalent period for the earlier PSK comparator calibration, this totals 60 hours for measuring the two grids on the PSK. The lengthier PSK measurement time is due to its inherent double-pointing requirement (Schwidefsky 1960) (object pointing and then nearest PSK-grid-intersection pointing) and to the fact that totally independent pointings (repetitions) were made on the PSK whereas the Mann comparator measurements were replicative (International Society for Photogrammetry 1964).

The pointing precision for each case of measurements was computed by:

$$m_x = \sqrt{\frac{\sum_{j=1}^p \left\{ \sum_{i=1}^t (x_i - \bar{x}_j) \right\}^2}{N - p}} \quad (3)$$

$$m_{pt} = \sqrt{\frac{m_x^2 + m_y^2}{2}} \quad (4)$$

where: $N = \sum_{j=1}^p (n_j) =$ total number of pointings,

$t_j =$ total number of pointings of intersection j ,

$p =$ total number of grid intersections.

Since the various operators demonstrated unequal pointing skills (table 1), the inverse pointing precision variances of their measurements were applied as relative weights in step 6:

$$w_i = \frac{\bar{m}_{pt}^2}{m_{i,pt}^2} \quad (5)$$

where:

$$\bar{m}_{pt}^2 = \frac{\sum_{i=1}^n m_i^2}{n} \quad (6)$$

$n =$ total number of cases.

TABLE 1.—Comparator pointing precision (μm)

Case number	Operator	m_x	m_y	m_{pt}	Total number of pointings
Master grid 773—Mann comparator					
1	1	0.78	0.68	0.74	128
2		.65	.93	.80	129
3		.79	.72	.75	130
4		.92	.71	.83	128
Operator total*		.73	.71	.72	515
5	2	0.88	0.74	0.81	125
6		.89	.87	.88	125
7		.80	1.13	.98	135
8		.93	.84	.89	127
Operator total*		.81	.84	.82	512
9	3	0.69	0.54	0.62	126
10		.68	.57	.63	127
11		.63	.60	.62	125
12		.70	.50	.61	126
Operator total*		.62	.51	.57	504
Comparator total*		.71	.69	.70	1,531
New grid 1320—Mann comparator					
1	4	0.81	0.56	0.70	129
2		.64	.68	.66	130
3		.49	.67	.59	130
4		.57	.79	.69	135
Operator total*		.59	.63	.61	524
5	5	0.87	0.75	0.81	128
6		.70	.95	.84	130
7		.88	.74	.81	130
8		.84	.72	.78	128
Operator total*		.76	.73	.75	516
9	3	0.66	0.58	0.62	129
10		.65	.57	.61	127
11		.80	.50	.67	127
12		.64	.48	.57	126
Operator total*		.64	.49	.57	509
Comparator total*		.65	.62	.64	1,549
Master grid 773—PSK comparator					
1	6	1.26	0.78	1.05	123
2		.76	.89	.83	125
3		.65	.78	.72	125
4		.75	.77	.76	125
Operator total*		.81	.74	.78	498

TABLE 1.—Comparator pointing precision (μm)—
(Continued)

Case number	Operator	m_x	m_y	m_{pt}	Total number of pointings
Master grid 773—PSK comparator (continued)					
5	7	0.77	1.00	0.89	124
6		.79	1.21	1.02	125
7		.86	1.11	.99	125
8		.73	1.13	.95	125
Operator total*		.73	1.02	.89	499
9	8	0.96	0.94	0.95	125
10		.80	.93	.86	125
11		1.03	1.00	1.02	125
12		.79	.81	.80	125
Operator total*		.83	.85	.84	500
Comparator total*		.78	.86	.82	1,497
New grid 1320—PSK comparator					
1	9	1.48	1.37	1.43	145
2		1.22	1.37	1.30	150
3		1.32	1.63	1.49	143
4		1.44	1.32	1.38	148
Operator total*		1.27	1.33	1.30	586
5	10	0.87	0.77	0.82	119
6		1.01	.88	.95	125
7		.94	.87	.91	125
8		.92	.72	.83	150
Operator total*		.86	.75	.81	519
9	11	0.91	0.78	0.84	125
10		.88	.73	.80	125
11		.80	.85	.82	125
12		.88	.83	.86	125
Operator total*		.79	.73	.76	500
Comparator total*		1.00	.98	.99	1,605

*The lines designated Operator total and Comparator total are the pointing precision standard deviations of all pointings by the operator, or on the comparator. These deviations are computed under the assumption that all grid intersections are of equal quality and therefore may be pointed upon with equal precision by any operator, regardless of any 90° rotation of the intersection.

Table 2 presents the magnitude of the scale-smoothing process (step 7). The standard deviations (m_{c_i}) presented are computed from the differences between the previously orthogonalized mean-case coordinate values and

the provisional values chosen. In this test calibration, the provisional values chosen are the mean coordinates determined from the 12 orthogonalized cases of the PSK that are at the scale of the Master grid (773). The scale factors presented (table 2) show that the maximum variation between any two cases of a set is equivalent to 2.81 μm across the 20-cm plate before scaling. This scale discrepancy is readily explained considering a coefficient of thermal linear expansion of 1.3 $\mu\text{m}/20\text{ cm}/^\circ\text{F}$ for the Mann comparator (Mann 1966), the mean error of a PSK-grid intersection = $\pm 1.5\ \mu\text{m}$ (International Society for Photogrammetry 1960), the pointing precision of the comparators involved, and a least count readout of 1 μm for both Mann and PSK.

The grid calibration precision computed for each comparator (step 8, equations (1), (2)) presented as a standard deviation is:

12 cases (3 sets)	Before scaling		After scaling	
	$m_{\bar{c}}$	$\sigma_{m_{\bar{c}}}$	$m_{\bar{c}}$	$\sigma_{m_{\bar{c}}}$
Mann	$\pm 0.967\ \mu\text{m}$	$0.028\ \mu\text{m}$	$\pm 0.933\ \mu\text{m}$	$0.027\ \mu\text{m}$
PSK	$\pm 0.901\ \mu\text{m}$	$.027\ \mu\text{m}$	$\pm 0.852\ \mu\text{m}$	$.025\ \mu\text{m}$

The standard error of a standard deviation, $\sigma_{m_{\bar{c}}}$, indicates the reliability of the standard deviation as a function of the redundancy of observations (International Society for Photogrammetry 1960).

$$\sigma_{m_{\bar{c}}} = \frac{m_{\bar{c}}}{\sqrt{4n(p-1)}} = 0.029 m_{\bar{c}} \quad (7)$$

Because the dispersion of the individual case coordinate-determination variances (m_{c_i} in table 2) was deemed significant after scaling, relative weights were applied to the individual case coordinate determinations in the final computation of means (step 9) for both comparator grid-coordinate determinations.

$$w_{c_i} = \frac{m_{\bar{c}}^2}{m_{c_i}^2} \quad (8)$$

The coordinate values for grid 1320 as determined independently from: one trilateration set, three combined Mann comparator coordinate transfer sets, and three combined PSK comparator coordinate transfer sets, are presented in table 3.

TABLE 2.—Scale smoothing process

Case number	Mann comparator			PSK comparator		
	Unscaled m_{c_i} (μm)	Scaled m_{c_i} (μm)	Scale factor (m/m)*	Unscaled m_{c_i} (μm)	Scaled m_{c_i} (μm)	Scale factor (m/m)*
1	0.917	0.914	0.999998898	0.853	0.850	0.999999202
2	.872	.856	0.999997736	1.050	.839	1.000008777
3	.963	.957	1.000001561	1.090	1.089	1.000000670
4	.843	.843	1.000000332	.998	.896	1.000006146
5	1.299	1.232	0.999994281	.676	.654	0.999997614
6	.902	.896	1.000001553	.874	.873	0.999999372
7	.917	.913	1.000001077	.983	.931	0.999995636
8	1.189	1.026	1.000008322	.720	.686	1.000003102
9	.815	.726	0.999994879	.953	.952	0.999999319
10	.855	.846	1.000001756	.732	.701	1.000002987
11	.752	.750	1.000000867	.663	.661	1.000000600
12	1.121	1.112	1.000001933	1.067	.965	0.999993742
$m_{\bar{c}} =$.967	.933		.901	.852	

* m/m = meters per meter.

TABLE 3.—Coordinate values (μm)—grid 1320

Trilateration set

Point #	X	m_{x_i}	Y	m_{y_i}	m_{pt_i}
1	-100000.39	.493	-99999.01	.493	.493
2	-50000.25	.464	-100000.87	.477	.471
3	.97	.457	-99999.74	.485	.471
4	50000.61	.464	-100001.11	.477	.471
5	100000.94	.493	-100001.08	.493	.493
6	-99999.72	.477	-49999.07	.464	.471
7	-49999.48	.436	-50000.34	.436	.436
8	1.64	.434	-49999.81	.447	.441
9	50000.98	.436	-50001.38	.436	.436
10	99999.41	.477	-50002.65	.464	.471
11	-99999.15	.485	3.05	.457	.471
12	-49999.51	.447	1.08	.434	.441
13	3.21	.415	1.91	.415	.415
14	50000.94	.447	.85	.434	.441
15	99999.28	.485	.68	.457	.471
16	-100000.78	.477	50000.79	.464	.471
17	-50001.75	.436	49999.62	.436	.436
18	.68	.434	49999.85	.447	.441
19	50000.11	.436	49998.98	.436	.436
20	99998.65	.477	49999.41	.464	.471
21	-100001.51	.493	99999.72	.493	.493
22	-50000.38	.464	99999.65	.477	.477
23	-.24	.457	100000.88	.485	.471
24	49997.48	.464	99999.61	.477	.471
25	99998.22	.493	99998.95	.493	.493

$$m_o^2 = 1.140 \mu\text{m}$$

$$m_{pt} = .462$$

Weighted mean of three Mann comparator coordinate transfer sets—grid 1320

Point #	X	m_{x_i}	$m_{\bar{x}_i}$	Y	m_{y_i}	$m_{\bar{y}_i}$	m_{pt_i}	$m_{\bar{pt}_i}$
1	-99999.33	.837	.242	-99998.51	.746	.215	.793	.229
2	-50000.11	.720	.208	-99999.68	.839	.242	.781	.226
3	1.19	.863	.249	-99999.05	.457	.132	.690	.199
4	50002.26	.921	.266	-100001.22	.563	.162	.763	.220
5	100001.24	1.048	.303	-100001.98	.820	.237	.941	.272
6	-99998.51	.773	.223	-49999.43	.564	.163	.677	.195
7	-50000.25	.550	.159	-50000.35	.662	.191	.608	.176
8	1.04	.490	.141	-50000.59	.376	.108	.437	.126
9	50001.10	.825	.238	-50002.13	.756	.218	.791	.228
10	100000.53	.654	.189	-50003.15	.587	.169	.622	.179
11	-99998.96	.537	.155	3.38	.763	.220	.659	.190
12	-49999.54	.396	.114	1.50	.641	.185	.533	.154
13	1.93	.407	.118	1.99	.427	.123	.417	.120
14	50001.17	.574	.166	.73	.471	.136	.525	.152
15	100000.01	.763	.209	-.86	.545	.157	.640	.185

TABLE 3.—Coordinate values (μm)—grid 1320—Continued

Weighted mean of three Mann comparator coordinate transfer sets—grid 1320—Continued

Point #	X	m_{x_i}	$m_{\bar{x}_i}$	Y	m_{y_i}	$m_{\bar{y}_i}$	m_{pt_i}	$m_{\bar{pt}_i}$
16	-100001.21	.697	.201	50001.53	.644	.186	.671	.194
17	-50001.73	.628	.181	50000.22	.568	.164	.599	.173
18	.68	.608	.176	50000.52	.488	.141	.551	.159
19	49998.83	.593	.171	49999.74	.534	.154	.564	.163
20	99997.50	.607	.175	49999.04	.540	.156	.574	.166
21	-100001.24	.501	.145	100000.40	.673	.194	.593	.171
22	-50002.50	.707	.204	99999.64	.652	.188	.680	.196
23	.49	.689	.199	100000.32	.387	.112	.559	.161
24	49998.67	.688	.199	99999.09	.870	.251	.784	.226
25	99996.69	.853	.246	99998.83	.860	.248	.856	.247
Total		$m_x = .693$	$m_{\bar{x}} = .200$		$m_y = .634$	$m_{\bar{y}} = .183$	$m_{pt} = .664$	$m_{\bar{pt}} = .192$

Weighted mean of three PSK comparator coordinate transfer sets—grid 1320

1	-100000.28	.816	.235	-99999.05	.913	.263	.865	.250
2	-50000.58	.978	.282	-99999.96	.629	.182	.823	.237
3	.72	.725	.209	-99999.88	.754	.218	.740	.214
4	50001.07	.741	.214	-100000.72	.547	.158	.651	.188
5	100001.54	.900	.260	-100001.51	.782	.226	.843	.243
6	-99999.89	.841	.243	-49999.27	.911	.263	.877	.253
7	-50000.29	.694	.200	-50000.20	.929	.268	.820	.237
8	1.09	.532	.154	-50000.15	.710	.205	.627	.181
9	50000.72	.796	.230	-50001.13	.997	.288	.902	.260
10	99999.88	.934	.270	-50002.44	.735	.212	.841	.243
11	-99999.13	1.032	.298	2.45	.755	.218	.904	.261
12	-49999.40	.570	.164	1.17	.882	.255	.742	.214
13	2.66	.465	.134	2.06	.768	.222	.635	.183
14	50001.14	.737	.213	1.34	.856	.247	.799	.231
15	100000.16	.882	.255	.26	.620	.179	.763	.220
16	-100001.00	.560	.162	50000.69	.954	.275	.783	.226
17	-50001.33	.999	.288	49999.71	.724	.209	.872	.252
18	.76	.851	.246	50000.42	.755	.218	.805	.232
19	49998.81	1.032	.298	49999.32	.773	.223	.911	.263
20	99997.78	.989	.285	49999.07	.743	.214	.874	.252
21	-100001.00	.733	.211	99999.54	1.121	.324	.947	.273
22	-50001.05	.771	.223	99999.13	.937	.270	.858	.248
23	.73	.750	.216	100000.11	.845	.244	.799	.231
24	49998.85	.674	.194	99999.52	1.045	.302	.879	.254
25	99997.99	.957	.276	99999.54	.897	.259	.927	.268
Total		$m_x = .814$	$m_{\bar{x}} = .235$		$m_y = .834$	$m_{\bar{y}} = .241$	$m_{pt} = .824$	$m_{\bar{pt}} = .238$

For the trilateration coordinate set, table 3 shows the standard deviation of each coordinate (m_x, m_y, m_{pt}), the standard error of an observation of unit weight (m_o) as determined from the trilateration adjustment (Malhotra 1968, Poetzschke 1967), and the pooled standard deviation for a grid intersection (m_{pt}).

For each of the coordinate transfer coordinate sets, the standard deviation of a coordinate observation of unit weight ($m_{x_i}, m_{y_i}, m_{pt_i}$) and the standard deviation of the weighted mean coordinate ($m_{\bar{x}_i}, m_{\bar{y}_i}, m_{\bar{pt}_i}$) are listed in table 3. Also the pooled standard deviations (total $m_x, m_{\bar{x}}, m_y, m_{\bar{y}}, m_{pt}, m_{\bar{pt}}$) for a coordinate of a

set are given (under the premise that all x - and all y -coordinates of all grid intersections are of equal quality). These pooled statistics represent the grid calibration accuracy as determined from a single comparator. The standard deviation formulas for these statistics are:

For each grid intersection, the standard deviation of a coordinate (point) observation of unit weight is given by:

$$m_{x_i} = \sqrt{\frac{\sum_{i=1}^n \left\{ w_i (x_i - \bar{x}_w)^2 \right\}}{n-1}} \quad (9)$$

$$m_{y_i} = \sqrt{\frac{\sum_{i=1}^n w_i \left\{ (y_i - \bar{y}_w)^2 \right\}}{n-1}}$$

$$m_{pt_i} = \sqrt{\frac{\sum_{i=1}^n \left\{ w_i (x_i - \bar{x}_w)^2 + (y_i - \bar{y}_w)^2 \right\}}{2(n-1)}} \quad (10)$$

$$= \sqrt{\frac{m_{x_i}^2 + m_{y_i}^2}{2}}$$

and the standard deviation of a weighted mean coordinate (at a particular intersection) is given by:

$$m_{\bar{x}_i} = \sqrt{\frac{\sum_{i=1}^n w_i (x_i - \bar{x}_w)^2}{\left\{ \sum_{i=1}^n w_i \right\} (n-1)}} \quad (11)$$

$$m_{\bar{y}_i} = \sqrt{\frac{\sum_{i=1}^n w_i (y_i - \bar{y}_w)^2}{\left\{ \sum_{i=1}^n w_i \right\} (n-1)}}$$

$$m_{p\bar{i}} = \sqrt{\frac{m_{\bar{x}_i}^2 + m_{\bar{y}_i}^2}{2}} \quad (12)$$

For these equations,

- n = total number of cases,
- w_i = i th case weight,
- p = total number of grid intersections.

For the grid, the standard deviation of a coordinate observation of unit weight is given by:

$$m_x = \sqrt{\frac{\sum_{i=1}^p \left\{ \sum_{j=1}^n [w_j (x_j - \bar{x}_w)^2] \right\}}{p(n-1)}} \quad (13)$$

$$m_y = \sqrt{\frac{\sum_{i=1}^p \left\{ \sum_{j=1}^n [w_j (y_j - \bar{y}_w)^2] \right\}}{p(n-1)}}$$

$$m_{pt} = \sqrt{\frac{m_x^2 + m_y^2}{2}} \quad (14)$$

and the standard deviation of weighted mean coordinate is given by:

$$m_{\bar{x}} = \sqrt{\frac{\sum_{i=1}^p \left\{ \sum_{j=1}^n [w_j (x_j - \bar{x}_w)^2] \right\}}{\left(\sum_{j=1}^n w_j \right) p(n-1)}} \quad (15)$$

$$m_{\bar{y}} = \sqrt{\frac{\sum_{i=1}^p \left\{ \sum_{j=1}^n [w_j (y_j - \bar{y}_w)^2] \right\}}{\left(\sum_{j=1}^n w_j \right) p(n-1)}}$$

$$m_{p\bar{t}} = \sqrt{\frac{m_{\bar{x}}^2 + m_{\bar{y}}^2}{2}} \quad (16)$$

ACCURACY DETERMINATION

The precision ($m_{\bar{c}}$) of the coordinate transfer technique for the test grid plate 1320 was shown to be $\pm 0.933 \mu\text{m}$ for the Mann comparator measurements and $\pm 0.852 \mu\text{m}$ for the PSK comparator measurements. The corresponding individual accuracies of the coordinate transfer values of grid 1320 are $\pm 0.664 \mu\text{m}$ for the Mann

measurements and $\pm 0.824 \mu\text{m}$ for the PSK measurements. The pooled standard error of a trilateration grid intersection is $\pm 0.462 \mu\text{m}$.

Since three independent determinations of the coordinates of grid 1320 were made, it would be desirable to compute a grand mean set of grid coordinates and its accuracy statistic. Also, to evaluate the accuracy of each of the individual determinations of grid coordinates, a statistical comparison of their values and a complete error propagation are required. The general development of grid accuracy formulas involves the following seven basic computation steps:

- (1) Determine the individual grid coordinate sets (x_i).
- (2) Compute the grand mean-coordinate set (\bar{x}).

Note: If the accuracies of the individual grid coordinate determinations are known a priori, then the grand weighted mean-coordinate set (\bar{X}) should be computed, using reciprocal variances as weights. Following this computation, proceed with only the computations outlined in steps 3, 4, and 7, using weights and the grand weighted mean.

- (3) Compute the variance of differences ($\sigma_{d_i}^2$) between the individual grid coordinate sets and the grand mean-coordinate set.
- (4) Determine the accuracy of each independent coordinate set (σ_{x_i}).
- (5) Determine the accuracy of the grand mean-coordinate set ($\sigma_{\bar{x}}$).
- (6) Compute the grand weighted mean-coordinate set (\bar{X}).
- (7) Determine the accuracy of the grand weighted mean-coordinate set ($\sigma_{\bar{X}}$).

When only two independent determinations of the coordinates of a grid have been made, the grand mean-coordinate set should be computed. Its accuracy statistic is the pooled standard deviation of both independent sets from the grand mean-coordinate set.

When three or more independent determinations of the coordinates of a grid have been made, the seven basic steps outlined above must be followed. Development of the error propagation formulas involved in these steps is a complex problem. Because of the unusual character of this problem, neither matrix nor conventional notation alone conveniently describes the mathematical operations performed. Therefore, several of the seven computation steps are derived in either or both notations.

Nota Bene: Conventional equation numbers include a small letter, and the corresponding matrix equation number includes the corresponding capital letter; for

example, (17a) refers to the conventional notation equation whose counterpart matrix equation is denoted (17A).

Grid Accuracy Formula Development

Let: k = the number of independent grid coordinate sets.

x_i = the grid coordinates of an independent set.

w_i = the weight assigned to the independent coordinate set x_i .

X = a column vector of the independent coordinate sets, k sets in length.

W = a diagonal matrix containing the weights assigned to the independent coordinate sets of X .

E = a column vector of units, k units in length.

$$X = \begin{bmatrix} x_1 \\ x_2 \\ x_3 \\ \vdots \\ \vdots \\ \vdots \\ x_k \end{bmatrix} \quad E = \begin{bmatrix} 1 \\ 1 \\ 1 \\ \vdots \\ \vdots \\ \vdots \\ 1 \end{bmatrix}_k \quad W = \begin{bmatrix} w_1 & 0 & 0 & \dots & 0 \\ 0 & w_2 & 0 & \dots & 0 \\ 0 & 0 & w_3 & \dots & 0 \\ \vdots & \vdots & \vdots & \ddots & \vdots \\ \vdots & \vdots & \vdots & \vdots & \ddots \\ 0 & 0 & 0 & \dots & w_k \end{bmatrix}_{k,k}$$

- (1) Determine the individual grid coordinate sets (x_i).

For example, for grid 1320, Mann = x_1 , PSK = x_2 , trilateration = x_3 . These coordinate sets are given in table 3.

- (2) Compute the grand mean-coordinate set (\bar{x}) by means of equation (17), using unit weights.

$$\bar{x} = \frac{\sum_{i=1}^k (w_i x_i)}{\sum_{i=1}^k (w_i)} \quad (17a)$$

$$\bar{X} = (E'WE)^{-1} E'WX \quad (17A)$$

The accuracy of the grand mean-coordinate set ($\sigma_{\bar{x}}$) is derived by applying the general law of error propagation:

$$\sigma_{\bar{x}}^2 = \frac{1}{\sum_{i=1}^k (w_i)} \sum_{i=1}^k (w_i^2 \sigma_{x_i}^2) \frac{1}{\sum_{i=1}^k (w_i)} \quad (18a)$$

$$\sum_{\bar{X}} = (E'WE)^{-1} E'W^2 \sum_X E (E'WE)^{-1}. \quad (18A)$$

Note: $(E'WE)^{-1}$ is a scalar = $\frac{1}{\sum_{i=1}^k (w_i)}$

and $\sum_{\bar{X}} = \sigma_{\bar{X}}^2$ is a 1 by 1.

Therefore,

$$\sigma_{\bar{X}}^2 = \left\{ \sum_{i=1}^k (w_i) \right\}^{-2} \sum_{i=1}^k (w_i^2 \sigma_{x_i}^2) \quad (18b)$$

$$\sum_X = (E'WE)^{-2} E'W^2 \sum_X E. \quad (18B)$$

- (3) Compute the variance of differences ($\sigma_{d_i}^2$) between individual grid coordinate sets and the grand mean-coordinate set by

$$d_i = x_i - \bar{x} \quad (19a)$$

$$D = X - E\bar{X}. \quad (19A)$$

The variance of differences for each coordinate set is computed using equation (1), replacing m_c^2 with $\sigma_{d_i}^2$. However, to provide a basis for the formula development of the accuracy of the individual coordinate set determinations, the following equation expansion and error propagation is required:

From equations (17A) and (19A):

$$D = X - E(E'WE)^{-1} E'WX.$$

Since $(E'WE)^{-1}$ is a scalar, this may be rewritten as

$$D = [I - (E'WE)^{-1} EE'W]X. \quad (19B)$$

or $D = GX$,

where $G = [I - (E'WE)^{-1} EE'W]X$

Note: G is idempotent and therefore singular.

By error propagation of equation (19B),

$$\sum_D = G \sum_X G', \quad (20A)$$

or propagated from equation (19a),

$$\sigma_{d_i}^2 = \sigma_{x_i}^2 + \sigma_{\bar{x}}^2 - 2\sigma_{x\bar{x}}. \quad (20a)$$

- (4) Determine the accuracy of each independent coordinate set (σ_{x_i}).

Equation (17a) is a function of the general form $y = gx$. By error propagation, the covariance of function y with parameters x is $\sigma_{yx} = g \sigma_x^2$. Therefore, the covariance of x_i with \bar{x} for equation (17a) is:

$$\sigma_{x_i \bar{x}} = \frac{1}{\sum_{i=1}^k (w_i)} (w_i \sigma_{x_i}^2). \quad (21a)$$

The expanded form of the variance of differences, equation (20b), is obtained by substituting equations (18a) and (21a) into equation (20a).

$$\sigma_{d_i}^2 = \sigma_{x_i}^2 + \left\{ \sum_{i=1}^k (w_i) \right\}^{-2} \sum_{i=1}^k (w_i \sigma_{x_i}^2) \quad (20b)$$

$$- 2 \left\{ \sum_{i=1}^k (w_i) \right\}^{-1} (w_i \sigma_{x_i}^2).$$

A solution for σ_{x_i} in this equation form is not apparent and the solution for \sum_X in equation (20A) is indeterminate due to the singularity of G . Therefore, a parallel matrix derivation of equation (20b) is presented. The diagonal elements of \sum_D are known by computation using equation (1). Since \sum_X is a diagonal matrix, because of the independence of coordinate set determinations, an alternative matrix approach is used, with column vectors for the diagonal elements of \sum_D , \sum_X , and $\sum_{X\bar{X}}$ (denoted by \sum_D^v , \sum_X^v , and $\sum_{X\bar{X}}^v$).

Equation (20a), rewritten in matrix column notation is:

$$\sum_D^v = \sum_X^v + E \sum_{\bar{X}} - 2 \sum_{X\bar{X}}^v. \quad (20A')$$

Equation (18B) in matrix column notation is:

$$\sum_{\bar{X}} = (E'WE)^{-2} E' W^2 \sum_X^v. \quad (18B')$$

By error propagation of equation (17A), the covariance of the function is:

$$\sum_{X\bar{X}}^v = (E'WE)^{-1} W \sum_X^v. \quad (21A)$$

Substituting equations (18B') and (21A) into equation (20A'), we obtain

$$\begin{aligned} \sum_D^v &= \sum_X^v + E(E'WE)^{-2} E W^2 \sum_X^v \\ &\quad - 2(E'WE)^{-1} W \sum_X^v, \end{aligned} \quad (20B)$$

which, after simplifying by collecting common terms, becomes

$$\sum_D^v = \left\{ I + (E'WE)^{-2} EE'W^2 - 2(E'WE)^{-1} W \right\} \sum_X^v. \quad (20C)$$

An inspection of the coefficient matrix of equation (20C) reveals that it is composed of the squared elements of the matrix G (see equation 19B) and therefore could have been derived directly from the expanded form of equation (20A).

Equation (20C) can be solved uniquely for the individual coordinate set variances ($\sigma_{x_i}^2$, \sum_X^v), as there are k equations containing k unknown variances.

Let:

$$F = I + (E'WE)^{-2} EE'W^2 - 2(E'WE)^{-1} W \quad (22)$$

$$\sum_D^v = F \sum_X^v \quad (20D)$$

Therefore,

$$\sum_X^v = F^{-1} \sum_D^v + H^v, \quad (23)$$

where the additional term (H^v) represents the known variance of the master grid coordinates used in the coordinate transfer sets. For "null" method determination values, for example, trilateration values, this term is zero.

Because of the patterned structure of F , a simplification in the inverse computation is possible as follows:

$$\begin{aligned} F &= [W^{-2} - 2(E'WE)^{-1} W^{-1} \\ &\quad + (E'WE)^{-2} EE'] W^2. \end{aligned}$$

Let

$$S = W^{-2} - 2(E'WE)^{-1} W^{-1}$$

Note: S is diagonal and therefore easily inverted.)

$$F = [S + (E'WE)^{-2} EE'] W^2$$

$$F^{-1} = W^{-2} [S + (E'WE)^{-2} EE']^{-1}$$

By matrix identity:

$$\begin{aligned} &[S + (E'WE)^{-2} EE']^{-1} \\ &= S^{-1} + S^{-1} E [- (E'WE)^2 - E'S^{-1} E]^{-1} E'S^{-1}. \end{aligned}$$

Note: $E' S^{-1} E$ is a scalar.

Hence,

$$\begin{aligned} F^{-1} &= W^{-2} S^{-1} \left\{ I - [(E'WE)^2 \right. \\ &\quad \left. + E' S^{-1} E]^{-1} EE' S^{-1} \right\}. \end{aligned}$$

The error propagation may be further simplified when $W = I$, as $E'WE = k$, and therefore equation (22) becomes

$$F = I + \frac{1}{k^2} EE' W^2 - \frac{2}{k} W.$$

Therefore,

$$F = \frac{1}{k^2} \{ (k^2 - 2k)I + EE' \}, \quad (24)$$

which is a k -square matrix of the following form:

$$F = \frac{1}{k^2} \begin{bmatrix} (k-1)^2 & 1 & 1 & \dots & 1 \\ 1 & (k-1)^2 & 1 & \dots & 1 \\ 1 & 1 & (k-1)^2 & \dots & 1 \\ \dots & \dots & \dots & \dots & \dots \\ \dots & \dots & \dots & \dots & \dots \\ 1 & 1 & 1 & \dots & (k-1)^2 \end{bmatrix}$$

This is a super symmetric matrix whose inverse form is:

$$F^{-1} = \frac{1}{(k-2)(k-1)} \{ k(k-1)I - EE' \}. \quad (25)$$

Therefore, the simplified version of equation (23), when $W = I$, is:

$$\sum_X^v = \frac{1}{(k-2)(k-1)} \{ k(k-1)I - EE' \} \sum_D^v + H^v. \quad (26)$$

- (5) Determine the accuracy of the grand mean-coordinate set ($\sigma_{\bar{x}}$).

Since unit weights are used to compute the grand mean-coordinate set, the accuracy equations (18b) and (18B') may be simplified to:

$$\sigma_{\bar{x}}^2 = \frac{1}{k^2} \sum_{i=1}^k (\sigma_{x_i}^2) \quad (18c)$$

$$\sum_{\bar{X}} = (E'E)^{-2} E' \sum_X^v. \quad (18C)$$

- (6) Compute the grand weighted mean-coordinate set (\bar{X}).

The reciprocal of the variance of each independent coordinate set, as determined by equa-

tion (23) or (26) of step 4, is the appropriate set weight to be applied in equation (17a) or (17A) to obtain X .

- (7) Determine the accuracy of the grand weighted mean-coordinate set ($\sigma_{\bar{X}}$).

This value is computed using the appropriate set weights in equation (18b) or (18B').

Accuracy Determination for Grid 1320

For grid 1320 the individual grid coordinate sets are given in table 3 and the grand mean coordinate set (\bar{x} of step 2) is presented in table 4. Weight one was initially chosen as the most appropriate weight for the combination of one trilateration set and two independent coordinate transfer sets. The variance vector (\sum_D^v of step 3) of differences between the independent coordinate sets and the grand mean was computed from the values presented in tables 3 and 4 using equation (1).

The variance vector (\sum_X^v of step 4) of each independent coordinate set was computed as follows:

$$\text{Given: } k = 3 \\ W = I$$

$$\sum_D^v = F \sum_X^v \quad (20D)$$

$$\sum_D^v = \begin{bmatrix} \sigma_{M-\bar{x}}^2 \\ \sigma_{P-\bar{x}}^2 \\ \sigma_{T-\bar{x}}^2 \end{bmatrix}$$

$$= \begin{bmatrix} 0.20521 \\ 0.07529 \\ 0.16764 \end{bmatrix} = \frac{1}{9} \begin{bmatrix} 4 & 1 & 1 \\ 1 & 4 & 1 \\ 1 & 1 & 4 \end{bmatrix} \begin{bmatrix} \sigma_M^2 \\ \sigma_P^2 \\ \sigma_T^2 \end{bmatrix}$$

where:

M = Mann comparator set of coordinates.

P = PSK set of coordinates.

T = Trilateration set of coordinates.

\bar{x} = Grand mean set of coordinates.

Solution:

$$\sum_X^v = F^{-1} \sum_D^v + H^v. \quad (23)$$

$$\begin{aligned} \sum_X^v &= \begin{bmatrix} \sigma_M^2 \\ \sigma_P^2 \\ \sigma_T^2 \end{bmatrix} \\ &= \frac{1}{2} \begin{bmatrix} 5 & -1 & -1 \\ -1 & 5 & -1 \\ -1 & -1 & 5 \end{bmatrix} \begin{bmatrix} 0.20521 \\ 0.07528 \\ 0.16764 \end{bmatrix} + \begin{bmatrix} .09 \\ .09 \\ 0 \end{bmatrix} \\ &= \begin{bmatrix} 0.48156 \\ 0.09178 \\ 0.27886 \end{bmatrix} \end{aligned}$$

Note: the value 0.09 represents the variance of the master grid 773 that was used in the Mann and PSK coordinate transfers.

The grand weighted mean-coordinate set (\bar{X} of step 6) computed is given in table 5. The reciprocals of the computed \sum_X^v were the appropriate weights used. The accuracy of both mean coordinate sets (\bar{x} of step 2 and \bar{X} of step 6) was computed by equation (18B').

In summary, the accuracy of the determination of grid 1320 is indicated by the following standard errors:

- 0.694 μm for the Mann comparator set,
- 0.303 μm for the Zeiss PSK set,
- 0.528 μm for the trilateration set,
- 0.308 μm for the grand mean set,
- 0.246 μm for the grand weighted mean set.

The fact that these accuracy determinations are significantly lower than the grid precision determinations ($m_{\bar{x}}$) is very rewarding as it demonstrates the absence of significant biases in the various independent methods.

A graphic display of these final coordinate sets is presented in figures 1 and 2. In figure 1, the reference reseau represents the manufacturer's intended "square" grid intersections. Note the generally parallel trend created by the nonlinear path of the engraving tool in

TABLE 4.—Grand mean-coordinate set for grid 1320

Point #	X	m_x	$m_{\bar{x}}$	Y	m_y	$m_{\bar{y}}$	m_{pt}	$m_{\bar{pt}}$
1	-99999.99	.586	.338	-99998.85	.298	.172	.465	.268
2	-50000.31	.240	.139	-100000.17	.622	.359	.472	.272
3	.96	.235	.136	-99999.56	.444	.257	.355	.205
4	50001.31	.846	.488	-100001.02	.263	.152	.626	.362
5	100001.23	.295	.170	-100001.52	.450	.260	.381	.220
6	-99999.37	.755	.436	-49999.25	.176	.101	.548	.316
7	-50000.00	.451	.260	-50000.29	.087	.050	.325	.187
8	1.25	.336	.194	-50000.18	.386	.223	.362	.209
9	50000.93	.196	.113	-50001.54	.515	.297	.389	.225
10	99999.93	.558	.322	-50002.75	.365	.211	.471	.272
11	-99999.08	.102	.059	2.95	.472	.273	.342	.197
12	-49999.48	.070	.040	1.24	.217	.125	.161	.093
13	2.60	.642	.370	.198	.075	.043	.457	.264
14	50001.08	.125	.072	.97	.317	.183	.241	.139
15	99999.81	.467	.270	.03	.791	.456	.649	.375
16	-100000.99	.210	.121	50001.00	.462	.267	.359	.207
17	-50001.60	.243	.140	49999.85	.324	.187	.286	.165
18	.70	.049	.028	50000.26	.356	.205	.254	.147
19	49999.25	.748	.432	49999.34	.381	.220	.593	.343
20	99997.97	.601	.347	49999.17	.211	.122	.451	.260
21	-100001.24	.260	.150	99999.88	.457	.264	.372	.215
22	-50001.30	1.079	.623	99999.47	.300	.173	.792	.457
23	.32	.504	.291	100000.43	.402	.232	.456	.263
24	49998.33	.741	.428	99999.40	.284	.164	.561	.324
25	99997.63	.829	.478	99999.10	.378	.218	.644	.372
Total		$m_x = .526$	$m_{\bar{x}} = .303$		$m_y = .393$	$m_{\bar{y}} = .227$	$m_{pt} = .464$	$m_{\bar{pt}} = .268$

TABLE 5.—Grand weighted mean-coordinate set for grid 1320

Point #	X	m_x	$m_{\bar{x}}$	Y	m_y	$m_{\bar{y}}$	m_{pt}	$m_{\bar{pt}}$
1	-100000.18	.402	.232	-99998.97	.212	.123	.321	.186
2	-50000.44	.224	.129	-100000.12	.494	.285	.384	.222
3	.83	.207	.119	-99999.75	.330	.190	.275	.159
4	50001.12	.572	.330	-100000.87	.253	.146	.442	.255
5	100001.36	.298	.172	-100001.47	.315	.182	.307	.177
6	-99999.67	.549	.317	-49999.25	.128	.074	.399	.230
7	-50000.10	.401	.231	-50000.24	.087	.050	.290	.167
8	1.20	.283	.164	-50000.12	.267	.154	.275	.159
9	50000.82	.184	.106	-50001.31	.396	.229	.309	.178
10	99999.85	.384	.222	-50002.57	.286	.165	.339	.196
11	-99999.11	.070	.040	2.69	.437	.252	.313	.181
12	-49999.44	.069	.040	1.18	.147	.085	.115	.066
13	2.68	.445	.257	2.02	.076	.044	.319	.184
14	50001.10	.104	.060	1.15	.307	.177	.229	.132
15	99999.94	.431	.249	.21	.534	.309	.486	.280
16	-100000.98	.150	.087	50000.81	.338	.195	.262	.151
17	-50001.46	.246	.142	49999.75	.220	.127	.233	.135
18	.73	.049	.028	50000.30	.293	.169	.210	.121
19	49999.09	.655	.378	49999.29	.264	.152	.499	.288
20	99997.93	.478	.276	49999.13	.179	.104	.361	.208
21	-100001.13	.261	.151	99999.68	.347	.200	.307	.177
22	-50001.08	.731	.422	99999.30	.304	.175	.560	.323
23	.49	.480	.277	100000.30	.386	.223	.435	.251
24	49998.52	.676	.390	99999.48	.193	.111	.497	.287
25	99997.87	.564	.326	99999.32	.367	.212	.476	.275
Total		$m_x = .407$	$m_{\bar{x}} = .235$		$m_y = .308$	$m_{\bar{y}} = .178$	$m_{pt} = .361$	$m_{\bar{pt}} = .209$

both x and y directions. The variations in the engraving tool spacing are also discernible. Figure 2 portrays the same data referenced to the grand weighted mean set as the reseau. This is essentially a graphic representation of the standard errors given above, broken down into their individual grid locations. Table 5 shows these individual grid location standard errors.

Trilateration set	Standard error μm
1	± 0.955
2	± 1.132
3	$\pm .580$
4	$\pm .791$
5	$\pm .682$
Grand weighted mean	$\pm .382$

GRID 773—A TRILATERATION COMPARISON

As previously mentioned, grid 773 was chosen as a master grid for the coordinate transfer of grid 1320. To provide the reader with a realistic comparison and evaluation of the relative merits of both methods, an accuracy computation, as outlined in the previous section, was performed on the five trilaterations of grid 773. For each trilateration set, a relative weight was computed equal to the reciprocal of the trilateration adjustment variance of an observation of unit weight. The resultant accuracies, portrayed as standard errors, are as follows:

Plots of these coordinate sets are shown in figures 3 and 4, with the reference reseaus representing the manufacturer's intended square grid intersections in figure 3 and the reference reseaus representing the grand weighted mean set of values in figure 4. These plots correspond to figures 1 and 2 for the coordinate transfer method. The reader should note that although the coordinate transfer method provides more consistent results, it is not a replacement method for trilateration of grids but rather an efficient, less costly successor to an initial trilateration.

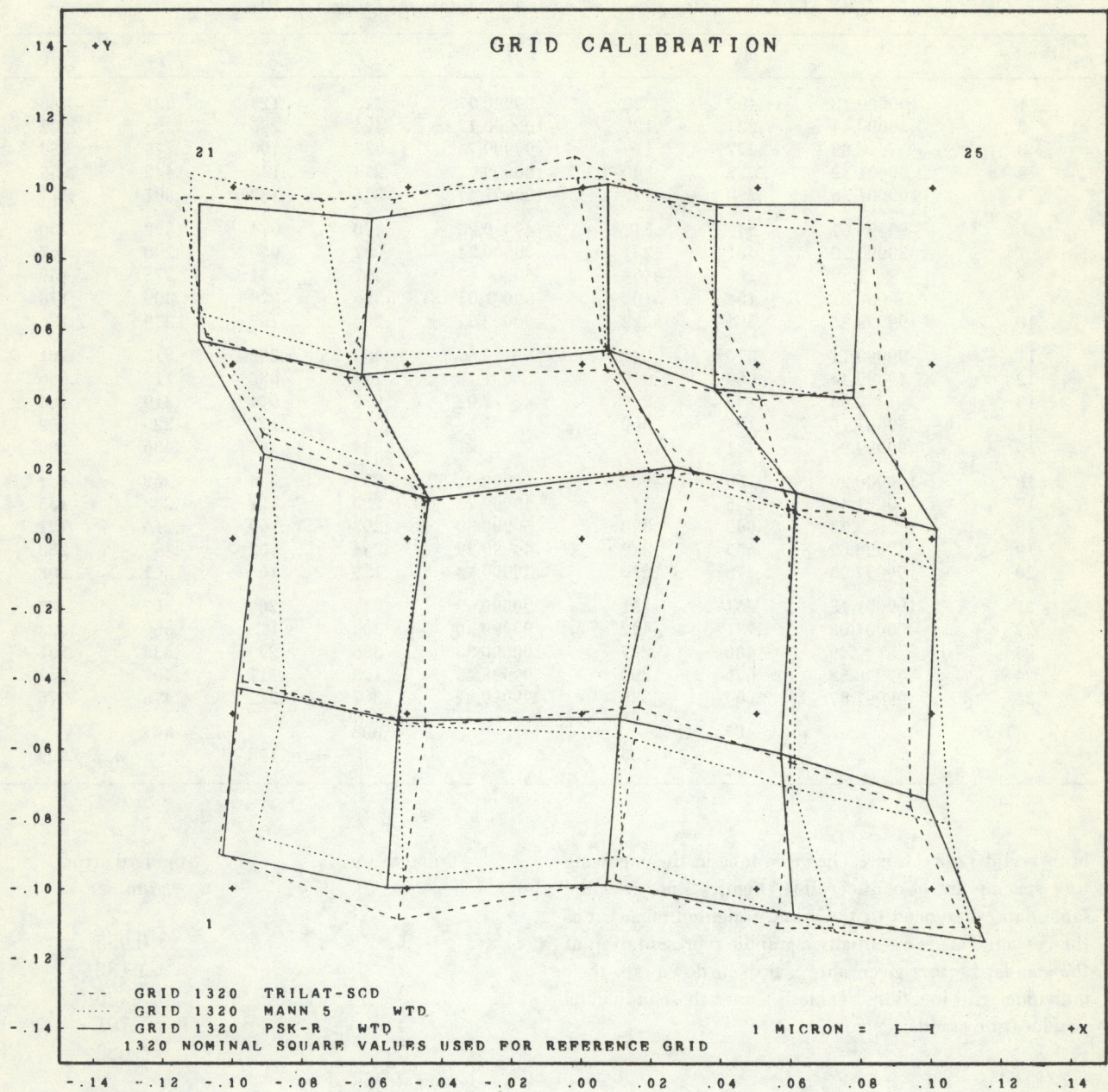


FIGURE 1.—Three independent determinations of grid 1320 referenced to the manufacturer's intended square reseau.

GRID CALIBRATION

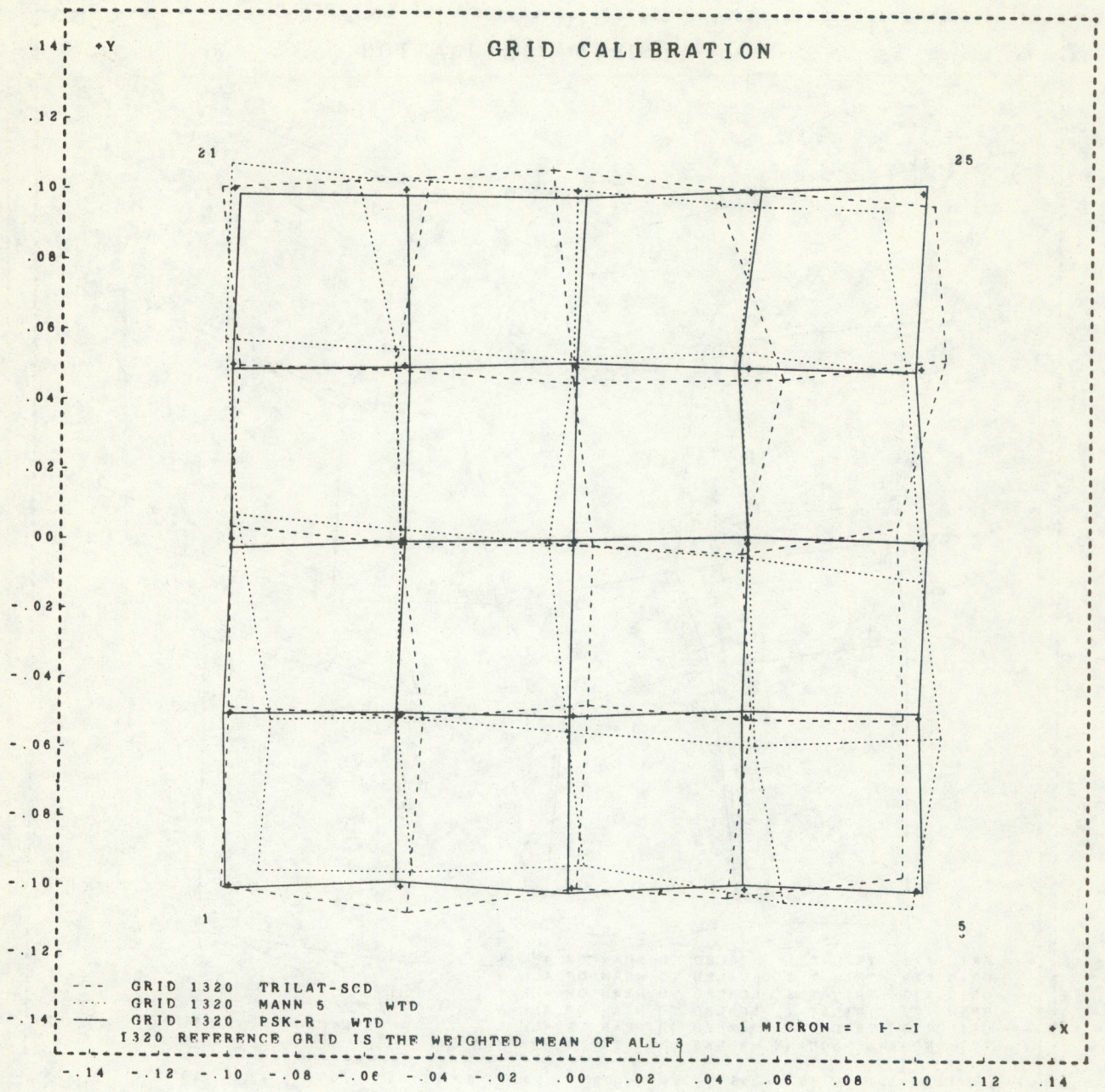


FIGURE 2.—Differences between three independent determinations of grid 1320 referenced to their grand weighted mean-coordinate set.

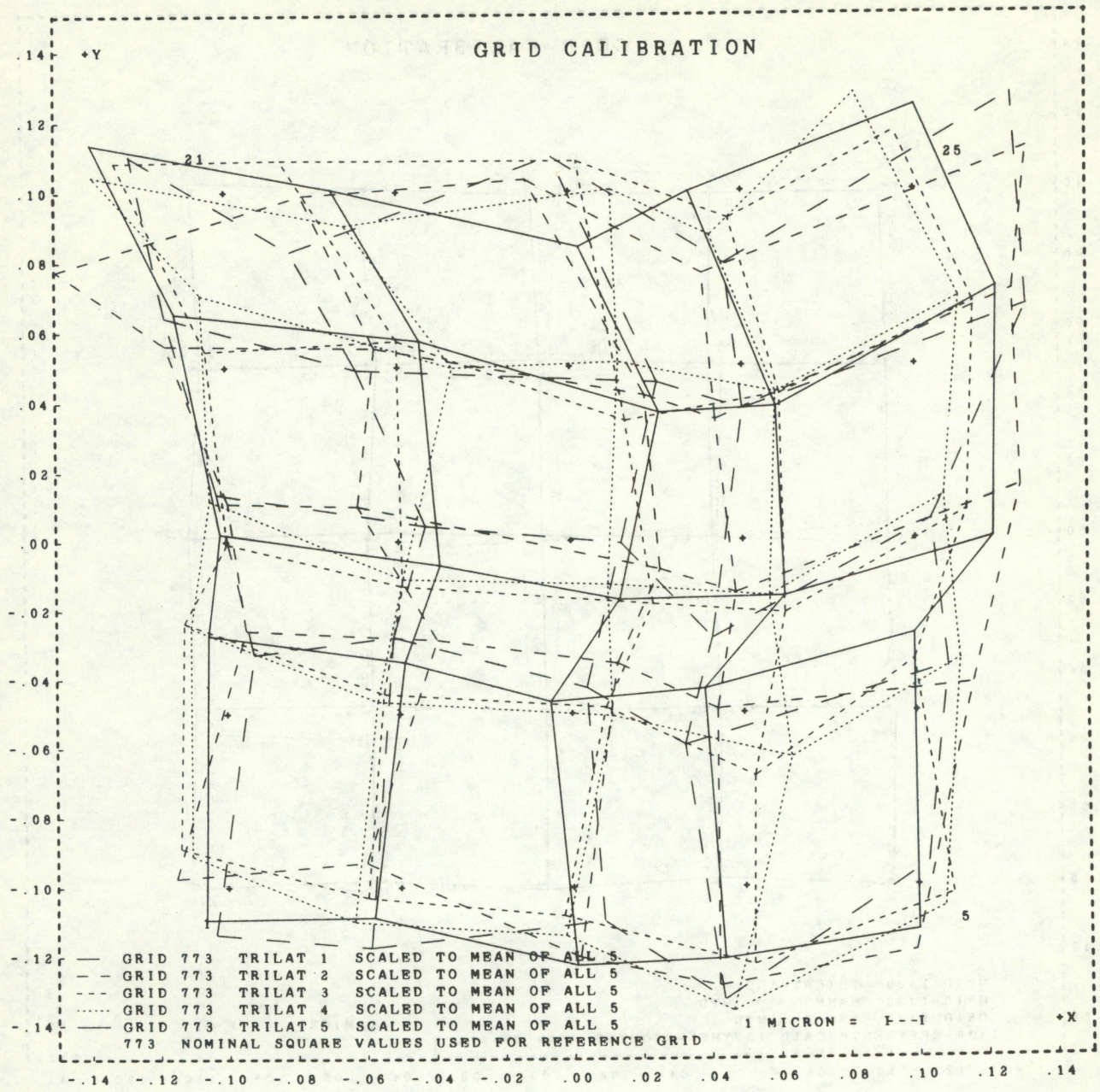


FIGURE 3.—Five trilateration determinations of grid 773 referenced to the manufacturer's intended square reseau.

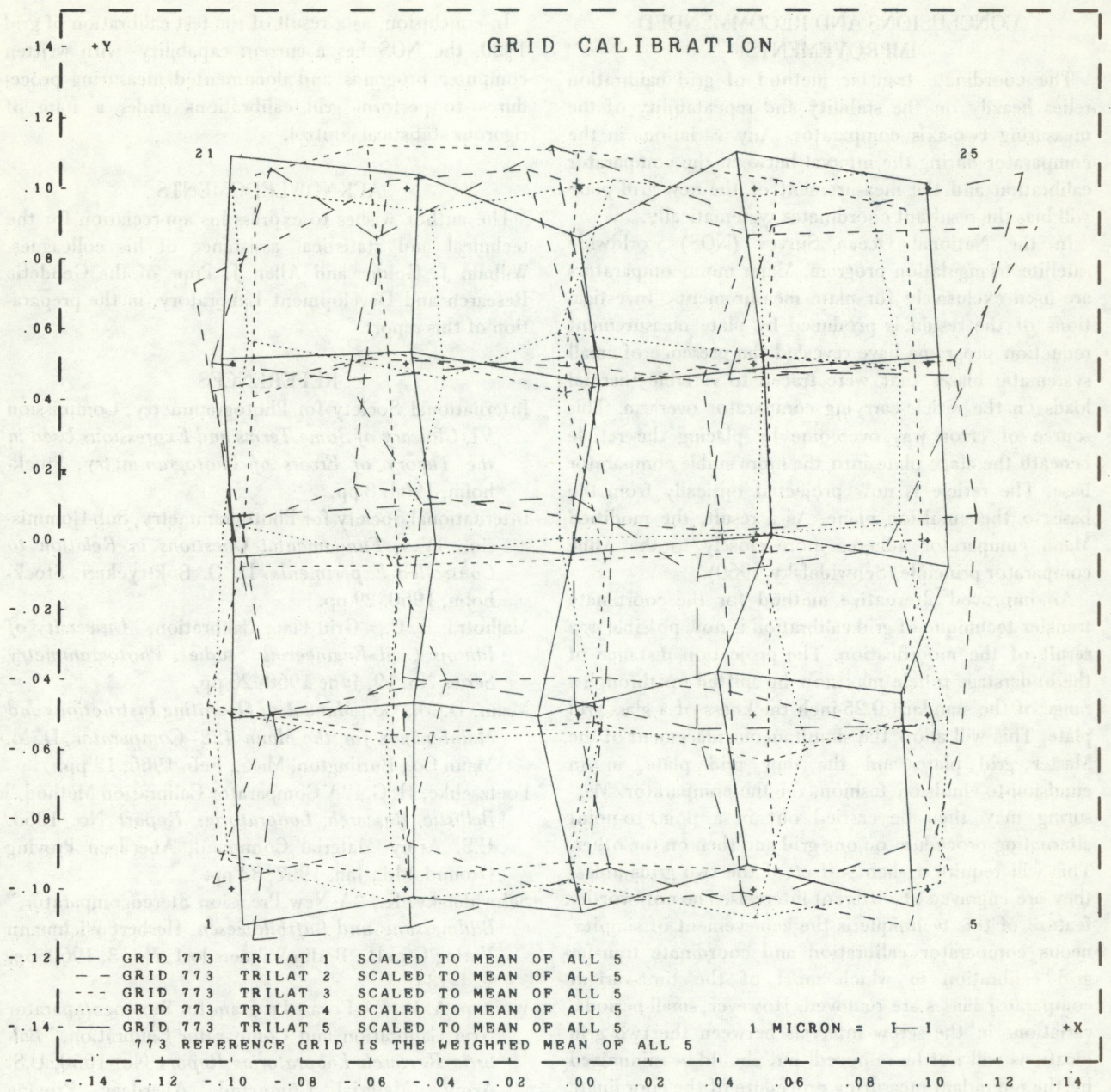


FIGURE 4.—Differences between five trilateration determinations of grid 773 referenced to their grand weighted mean-coordinate set.

CONCLUSIONS AND RECOMMENDED IMPROVEMENTS

The coordinate transfer method of grid calibration relies heavily on the stability and repeatability of the measuring two-axis comparator. Any variations in the comparator during the interval between the comparator calibration and the measurement of the new grid plate will bias the resultant coordinates systematically.

In the National Ocean Survey (NOS) worldwide satellite triangulation program, Mann monocomparators are used exclusively for plate measurements. Investigations of the residuals produced by plate measurement reduction programs have revealed the presence of small systematic biases that were traced to variable thermal loads on the reticle-carrying comparator overarm. This source of error was overcome by placing the reticle beneath the stage plate into the more stable comparator base. The reticle is now projected optically from the base to the emulsion plane. As a result, the modified Mann comparator adheres more closely to the Abbe comparator principle (Schwidersky 1960).

An improved alternative method for the coordinate transfer technique of grid calibration is now possible as a result of the modification. The projection distance of the understage reticle may now be shifted up through a range of the standard 0.25-inch thickness of a glass grid plate. This will allow the simultaneous placement of the Master grid plate and the new grid plate, in an emulsion-to-emulsion fashion, on the comparator. Measuring may then be carried out in a point-to-point alternating procedure on one grid and then on the other. This will require a slight offset of the two grids unless they are engraved at different intervals. The noteworthy feature of this technique is the achievement of simultaneous comparator calibration and coordinate transfer grid calibration in which most of the time-variant comparator biases are removed. However, small periodic variations in the screw intervals between the two grid locations will not be removed, but should be minimized by the redundant measuring procedure of the coordinate transfer method.

Another recommended improvement to coordinate transfer is to use the known variance of the Master grid plate in the data reduction adjustment programs, rather than to assume the Master grid is uniformly invariant.

In conclusion, as a result of the test calibration of grid 1320, the NOS has a current capability—with written computer programs and documented measuring procedures—to perform grid calibrations under a state of rigorous statistical control.

ACKNOWLEDGMENTS

The author wishes to express his appreciation for the technical and statistical assistance of his colleagues, William J. Golder and Allen J. Pope of the Geodetic Research and Development Laboratory, in the preparation of this report.

REFERENCES

- International Society for Photogrammetry, Commission VI, *Glossary of Some Terms and Expressions Used in the Theory of Errors of Photogrammetry*, Stockholm, 1964, 8 pp.
- International Society for Photogrammetry, Sub-Commission IV:4, *Fundamental Questions in Relation to Controlled Experiments*, H. O. Boktryckeri, Stockholm, 1960, 29 pp.
- Malhotra, R. C., "Grid Plate Calibration," *University of Illinois Civil Engineering Studies, Photogrammetry Series No. 19*, June 1968, 20 pp.
- Mann, D. M., Co., *Manual of Operating Instructions and Maintenance for the Mann 422-Comparator*, D. M. Mann Co., Burlington, Mass., Feb. 1966, 13 pp.
- Poetzschke, H. G., "A Comparator Calibration Method," *Ballistic Research Laboratories Report No. 1353*, U.S. Army Material Command, Aberdeen Proving Ground, Md., Jan. 1967, 33 pp.
- Schwidersky, K., "A New Precision Stereocomparator," *Bildmessung und Luftbildwesen*, Herbert Wichmann Verlag GmbH., Berlin-Wilmersdorf, No. 3, 1960, pp. 124-134.
- Wooten, A. R., "A Fortran Program for Stereocomparator Grid Calibration and Comparator Calibration," *Ballistic Research Laboratories Report No. 1600*, U.S. Army Material Command, Aberdeen Proving Ground, Md., Oct. 1964, 103 pp.
- Wooten, A. R., "A Fortran Program for Grid Calibration," *Ballistic Research Laboratories Memorandum Report No. 1742*, U.S. Army Material Command, Aberdeen Proving Ground, Md., Apr. 1966, 88 pp.

(Continued from inside front cover)

ESSA Technical Reports—C&GS

- *C&GS 32. Space Resection in Photogrammetry. M. Keller and G. C. Tewinkel, September 1966.
- *C&GS 33. The Tsunami of March 28, 1964, as Recorded at Tide Stations. M. G. Spaeth and S. C. Berkman, July 1967.
- *C&GS 34. Aerotriangulation: Transformation of Surveying and Mapping Coordinate Systems. Melvin J. Umbach, July 1967.
- *C&GS 38. Block Analytic Aerotriangulation. M. Keller and G. C. Tewinkel, November 1967.
- *C&GS 35. Geodetic and Grid Angles—State Coordinate Systems. Lansing G. Simmons, January 1968.
- *C&GS 36. Precise Echo Sounding in Deep Water. G. A. Maul, January 1969.
- *C&GS 37. Grid Values of Total Magnetic Intensity IGRF—1965. E. B. Fabiano and N. W. Peddie, April 1969.
- C&GS 39. An Advantageous, Alternative Parameterization of Rotations for Analytical Photogrammetry. Allen Pope, April 1970. Price \$0.30.
- C&GS 40. A Comparison of Methods of Computing Gravitational Potential Derivatives. L. J. Gulick, September 1970. Price \$0.40.

NOAA Technical Reports—NOS

- NOS 41. A User's Guide to a Computer Program for Harmonic Analysis of Data at Tidal Frequencies. R. E. Dennis and E. E. Long, July 1971. Price \$0.40.
- NOS 42. Computational Procedures for the Determination of a Simple Layer Model of the Geopotential From Doppler Observations. Bertold U. Witte, April 1971. Price \$0.65.
- NOS 43. Phase Correction for Sun-Reflecting Spherical Satellite, Erwin Schmid, July 1971. Price \$0.25.
- NOS 44. The Determination of Focal Mechanisms Using P- and S-Wave Data. William H. Dillinger, Allen J. Pope, and Samuel T. Harding, July 1971. Price \$0.60.
- NOS 45. Pacific SEAMAP 1961-70 Data for Area 15524-10. J. J. Dowling, E. F. Chiburis, P. Dehlinger, and M. J. Yellin, January 1972. Price \$3.50.
- NOS 46. Pacific SEAMAP 1961-70 Data for Area 15530-10. J. J. Dowling, E. F. Chiburis, P. Dehlinger, and M. J. Yellin, January 1972. Price \$3.50.
- NOS 47. Pacific SEAMAP 1961-70 Data for Area 15248-14. J. J. Dowling, E. F. Chiburis, P. Dehlinger, and M. J. Yellin, April 1972. Price \$3.50.
- NOS 48. Pacific SEAMAP 1961-70 Data for Area 16648-14. J. J. Dowling, E. F. Chiburis, P. Dehlinger, and M. J. Yellin, April 1972. Price \$3.00.
- NOS 49. Pacific SEAMAP 1961-70 Data for Areas 16530-10 and 17530-10. E. F. Chiburis, J. J. Dowling, P. Dehlinger, and M. J. Yellin, July 1972.
- NOS 50. Pacific SEAMAP 1961-70 Data for Areas 16524-10 and 17524-10. E. F. Chiburis, J. J. Dowling, P. Dehlinger, and M. J. Yellin, July 1972.
- NOS 51. Pacific SEAMAP 1961-70 Data for Areas 15636-12, 15642-12, 16837-12, and 16842-12. E. F. Chiburis, J. J. Dowling, P. Dehlinger, and M. J. Yellin, July 1972.
- NOS 52. Pacific SEAMAP 1961-70 Data Evaluation Summary. P. Dehlinger, E. F. Chiburis, and J. J. Dowling, July 1972.